Properties of scalar hairy black holes and scalarons with asymmetric potential

Xiao Yan Chew,[1,2,3,*] Dong-han Yeom,[2,3,5,†] and Jose Luis Blázquez-Salcedo[4,‡]

[1]*Department of Physics, School of Science, Jiangsu University of Science and Technology, 212100 Zhenjiang, Jiangsu Province, People's Republic of China*
[2]*Department of Physics Education, Pusan National University, Busan 46241, Republic of Korea*
[3]*Research Center for Dielectric and Advanced Matter Physics, Pusan National University, Busan 46241, Republic of Korea*
[4]*Departamento de Fśica Teórica and IPARCOS, Universidad Complutense de Madrid, E-28040 Madrid, Spain*
[5]*Leung Center for Cosmology and Particle Astrophysics, National Taiwan University, Taipei 10617, Taiwan*

(Received 12 October 2022; accepted 24 July 2023; published 8 August 2023)

This study explores the properties of black holes and scalarons in Einstein gravity when it is minimally coupled to a scalar field ϕ with an asymmetric potential $V(\phi)$, constructed in [A. Corichi *et al.*, Phys. Rev. D **73**, 084002 (2006)] a few decades ago. $V(\phi)$ has been applied in cosmology to describe the quantum tunneling process from the false vacuum to the true vacuum and contains a local maximum, a local minimum (false vacuum), and a global minimum (true vacuum). We focus on the asymptotically flat solutions, which can be constructed by appropriately fixing the local minimum of V. A branch of hairy black hole solutions emerges from the Schwarzschild black hole, and we study the domain of existence of such configurations. They can reach to a particlelike solution in the small horizon limit, i.e., the scalarons. We study the stability of black holes and scalarons, showing that all are unstable under radial perturbations.

DOI: 10.1103/PhysRevD.108.044020

I. INTRODUCTION

The "no hair" theorem states that the properties of black holes are only described by the mass, angular momentum and electrical charge after a gravitational collapse or by any dynamical perturbations of black holes as they approach the stationary limit. However, the no hair theorem can be circumvented under the right conditions. For example, the existence of particle-like solution for SU(2) Einstein-Yang-Mills theory shown by Bartnik and Mckinnon [1] had led to the construction of non-Abelian hairy black holes [2–6] which do not obey the no hair theorem anymore. One of the simplest ways to circumvent this theorem is to minimally couple Einstein gravity with a scalar field, introducing a scalar potential that is not strictly positive, such that the weak energy condition is violated [7]. In [8], spherically symmetric and asymptotically flat hairy black holes were constructed by employing a scalar potential that has a global minimum, local minimum, and local maximum (asymmetric potential). They obtained the asymptotically flat black holes by fixing the local minimum of potential to zero, to study the empirical mass formula of such black holes [8] and later generalize their model to a nonminimally coupled scalar field with gravity [9]. However, the properties of black holes, such as the Hawking temperature and mass, had not been investigated systematically in terms of the parameters of the scalar potential. In this work, we investigate the properties of these solutions by fixing the global minimum of the potential and varying the local maximum. This allows us to generate a branch of hairy black holes that bifurcate from the Schwarzschild black holes. See Refs. [10–18] for similar constructions of scalar hairy black holes.

When there is a scalar field with an asymmetric potential, quantum tunneling from a false vacuum (a local minimum) to a true vacuum (a global minimum) is allowed. With an $O(4)$-symmetric metric Ansatz, the Coleman-De Luccia instantons explain such a tunneling process via nucleation of a bubble [19]. If we extend the symmetry of the solution from $O(4)$-symmetry to the spherical symmetry, one can construct such solution within the Euclidean path integral formalism that explains the tunneling process [20,21]. For both cases, inside is a true-vacuum region, and after the nucleation, the bubble should expand over the spacetime; otherwise, the scalar field combination is, in general, unstable. Such a bubble may explain the phase transition of the early universe cosmology [22–27]; also, some interactions between bubbles may be a source of gravitational waves [28–30].

*xychew998@gmail.com
†innocent.yeom@gmail.com
‡jlblaz01@ucm.es

 © 2023 American Physical Society

However, the same solution can be interpreted as a kind of (unstable) scalaron or stationary hairy black hole solution. To provide a smooth field configuration at the horizon over the Euclidean manifold, one needs to provide a condition such that the derivative of the scalar field vanishes at the event horizon. On the other hand, if we generalize this boundary condition and focus only on the astrophysical aspects, it can still provide more generic boundary conditions [20,31]. This is the case that we will investigate.

This paper is organized as follows. In Sec. II, we briefly introduce our theoretical setup comprising the Lagrangian and the metric Ansatz. Then, we derive the set of coupled differential equations and study the asymptotic behavior of the functions. In Sec. III, we briefly introduce the quantities of interest for the black holes. In Sec. IV, we study the stability of the hairy black holes and scalarons by calculating the unstable mode of the radial perturbations of the metric and the scalar field. In Sec. V, we present and discuss our numerical findings. Finally, in Sec. VI, we summarize our work and present an outlook.

II. THEORETICAL SETTING

A. Theory and Ansätze

The action for Einstein gravity minimally coupled with an asymmetric potential $V(\phi)$ of a scalar field ϕ is given by [8]

$$S = \int d^4x\sqrt{-g}\left[\frac{R}{16\pi G} - \frac{1}{2}\nabla_\mu\phi\nabla^\mu\phi - V(\phi)\right], \quad (1)$$

where

$$V(\phi) = \frac{V_0}{12}(\phi-a)^2[3(\phi-a)^2 - 4(\phi-a)(\phi_0+\phi_1) + 6\phi_0\phi_1], \quad (2)$$

with a, V_0, ϕ_0 and ϕ_1 as constants. As exhibited in Fig. 1, the appearance of the cubic term ϕ^3 causes the potential to adopt an asymmetric shape. If the cubic term in the potential disappears, then the potential is Higgs-like, with two degenerate minima. Here, the constant a is the local minimum of the potential, ϕ_0 is the local maximum of the potential and ϕ_1 is the global minimum of the potential. Note that $0 < 2\phi_0 < \phi_1$. In cosmology, this potential can be used to explain the quantum tunneling process from a false vacuum a to a true vacuum ϕ_1.

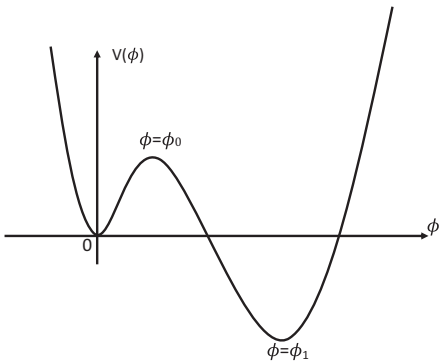

FIG. 1. An illustration of a generic asymmetric scalar potential $V(\phi)$.

The variation of the action with respect to the metric and scalar fields yields the Einstein and Klein-Gordon (KG) equations, respectively,

$$R_{\mu\nu} - \frac{1}{2}g_{\mu\nu}R = 8\pi G T_{\mu\nu}, \qquad \nabla_\mu\nabla^\mu\phi = \frac{dV(\phi)}{d\phi}, \quad (3)$$

where the stress-energy tensor $T_{\mu\nu}$ is given by

$$T_{\mu\nu} = -g_{\mu\nu}\left(\frac{1}{2}\nabla_\alpha\phi\nabla^\alpha\phi + V(\phi)\right) + \nabla_\mu\phi\nabla_\nu\phi. \quad (4)$$

We employ the following spherically symmetric Ansatz to construct the particle-like and black hole solutions;

$$ds^2 = -N(r)e^{-2\sigma(r)}dt^2 + \frac{dr^2}{N(r)} + r^2(d\theta^2 + \sin^2\theta d\varphi^2), \quad (5)$$

where $N(r) = 1-2m(r)/r$ and $m(r)$ is the Misner-Sharp mass function. It is important to note that $m(\infty) = M$ denotes, the total mass of the configuration.

B. Justification on the existence of the hairy black holes

In this section, we briefly justify the existence of the hairy black holes by referring to [7]. We multiply ϕ by the KG equation and integrate it from the black hole horizon to infinity,

$$\int_{r_H}^{\infty} d^4x\sqrt{-g}\left[\phi\nabla_\mu\nabla^\mu\phi - \phi\frac{dV(\phi)}{d\phi}\right] = 0. \quad (6)$$

We integrate the first term in the above expression by parts and obtain;

$$\int_{r_H}^{\infty} d^4x\sqrt{-g}\left[-\nabla_\mu\phi\nabla^\mu\phi - \phi\frac{dV(\phi)}{d\phi}\right] + \int_{\mathcal{H}} d^3\sigma n^\mu\phi\nabla_\mu\phi = 0, \quad (7)$$

where n^μ is the normal vector on the Killing horizon. The second term in the above expression is the boundary term that vanishes when we apply the boundary conditions for the scalar field at the horizon with $n^\mu\nabla_\mu\phi = 0$ and demand that the scalar field falls off at infinity. Hence, we are left with the following:

$$\int_{r_H}^{\infty} d^4x\sqrt{-g}\left[\nabla_\mu\phi\nabla^\mu\phi + \phi\frac{dV}{d\phi}\right] = 0. \quad (8)$$

Here, $\nabla_\mu\phi\nabla^\mu\phi \geq 0$ because the gradient of ϕ is perpendicular to both Killing vectors and thus has to be spacelike or zero. Subsequently, to obtain a regular and nontrivial hairy black hole, the term $\phi\frac{dV}{d\phi} \leq 0$. In our case, we choose ϕ to always be greater than zero, while the potential $V(\phi)$ is negative in some regions; the existence of nontrivial scalar hairy black holes is therefore allowed.

Furthermore, we can multiply the KG equation by $\frac{dV}{d\phi}$ and repeat the above procedure, obtaining the following:

$$\int_{r_H}^{\infty} d^4x\sqrt{-g}\left[\frac{d^2V}{d\phi^2}\nabla_\mu\phi\nabla^\mu\phi + \left(\frac{dV}{d\phi}\right)^2\right] = 0. \quad (9)$$

To make the terms in the square bracket vanish nontrivially, it is clear that $\frac{d^2V}{d\phi^2} < 0$, the condition that is also satisfied in our case. Note that in this derivation, it is not necessary to use the Einstein equation.

However, we can also see that the weak energy condition can be violated as V possesses a global minimum with $V < 0$ in some regions of ϕ;

$$\rho = -T_t^t = \frac{N}{2}\phi'^2 + V. \quad (10)$$

The violation of the weak energy condition leads to the violation of the strong energy condition (the opposite is not necessarily true). Moreover, we could also use the virial identity to reach the same conclusion, that is, $V \leq 0$ in some regions. However, for this analysis, it is necessary to introduce the metric Ansatz into the action.

In summary, this potential V possesses a local maximum and a global minimum which causes V to be negative in some regions. The local minimum at zero guarantees that the black hole is asymptotically flat. Moreover, it is possible to repeat the analysis to show the existence of solitonic solutions, just by changing the lower end of integration (no horizon with a fully regular spacetime).

C. Ordinary differential equations (ODEs)

By substituting Eq. (5) into the Einstein-matter field equation, we obtain a set of second-order and nonlinear ODEs for the metric functions,

$$m' = 2\pi Gr^2(N\phi'^2 + 2V), \qquad \sigma' = -4\pi Gr\phi'^2,$$
$$(e^{-\sigma}r^2N\phi')' = e^{-\sigma}r^2\frac{dV}{d\phi}, \quad (11)$$

where the prime denotes the derivative of the functions with respect to the radial coordinate r.

To construct globally regular black hole solutions, we need to know the asymptotic behavior of the functions at the horizon and the infinity. By making the series expansion for the functions at the horizon, the leading terms in the series expansion are given by the following:

$$m(r) = \frac{r_H}{2} + m_1(r - r_H) + O((r - r_H)^2), \quad (12)$$

$$\sigma(r) = \sigma_H + \sigma_1(r - r_H) + O((r - r_H)^2), \quad (13)$$

$$\phi(r) = \phi_H + \phi_{H,1}(r - r_H) + O((r - r_H)^2), \quad (14)$$

where

$$m_1 = 4\pi Gr_H^2V(\phi_H), \qquad \sigma_1 = -4\pi Gr_H\phi_{H,1}^2,$$
$$\phi_{H,1} = \frac{r_H\frac{dV(\phi_H)}{d\phi}}{1 - 8\pi Gr_H^2V(\phi_H)}. \quad (15)$$

Here, σ_H and ϕ_H are the values of σ and ϕ at the horizon. Similarly, the leading terms in the series expansion for scalaron at the origin are given by the following:

$$m(r) = \frac{4\pi GV(\phi_c)}{3}r^3 + O(r^5), \quad (16)$$

$$\sigma(r) = \sigma_c - \frac{\pi G}{9}\left(\frac{dV(\phi_c)}{d\phi}\right)^2 r^4 + O(r^8), \quad (17)$$

$$\phi(r) = \phi_c + \frac{1}{6}\frac{dV(\phi_c)}{d\phi}r^2 + O(r^4), \quad (18)$$

where σ_c and ϕ_c are the values of σ and ϕ at the origin, respectively.

Black holes and scalarons share the same asymptotic expansion of the metric and scalar functions at infinity. As we take $r \to \infty$, if we impose asymptotic flatness and the scalar field to vanish, then the leading terms are given by the following expressions:

$$m(r) = M + \tilde{m}_1\frac{\exp(-2m_{\text{eff}}r)}{r} + \cdots, \quad (19)$$

$$\sigma(r) = \tilde{\sigma}_1\frac{\exp(-2m_{\text{eff}}r)}{r} + \cdots, \quad (20)$$

$$\phi(r) = \bar{\phi}_{H,1}\frac{\exp(-m_{\text{eff}}r)}{r} + \cdots, \quad (21)$$

where $\tilde{m}_1$, $\tilde{\sigma}_1$, and $\tilde{\phi}_{H,1}$ are constants; and M is the total mass of the configuration. It is important to note that the effective mass of the scalar field is $m_{\text{eff}} = \sqrt{V_0\phi_0\phi_1}$.

We introduce the following dimensionless parameters;

$$r \to \frac{r}{\sqrt{4\pi G}}, \qquad m \to \frac{m}{\sqrt{4\pi G}}, \qquad \phi \to \sqrt{4\pi G}\phi. \quad (22)$$

The ODEs are solved by an ODE solver package Colsys which employs the Newton-Raphson method to solve the boundary value problem for a set of nonlinear ODEs by providing the adaptive mesh refinement to generate

the solutions to have more than 1000 points with high accuracy and the estimation of errors of solutions [32]. We compactify the radial coordinate r by $r = r_H/(1-x)$ for hairy black holes and $r = x/(1-x)$ for the scalaron in the numeric. Here we have five parameters $(\phi_H, \phi_0, \phi_1, V_0, r_H)$ to describe the hairy black holes and four parameters $(\phi_c, \phi_0, \phi_1, V_0)$ to describe the scalaron. To generate the solutions, we fix the global minimum ϕ_1, and the value of ϕ_0 is determined exactly when the boundary conditions are satisfied with the suitable choices of ϕ_c and ϕ_H for the scalaron and hairy black holes with fixed r_H and V_0, respectively.

When considering a hairy black hole, our solutions require a nonvanishing gradient of the scalar field at the event horizon. Therefore, if we maximally extend the causal structure over the Einstein-Rosen bridge (left of Fig. 2), one necessarily sees a cusp of the scalar field (black dashed curve) inside the horizon. In order to see this clearly, one can rewrite the scalar field configuration at the horizon [Eq. (14)] with the substitution $r = r_H/(1-y)$ where $-\infty < y < \infty$:

$$\phi(y) = \phi_H + r_H \phi_{H,1}\left(\frac{|y|}{1-|y|}\right) + O\left(\left(\frac{|y|}{1-|y|}\right)^2\right), \tag{23}$$

where $y < 0$ covers the left side of the Penrose diagram and $y > 0$ covers the right side of the Penrose diagram. Hence, a cusp appears at the horizon ($y = 0$). However, it is fair to say that our solutions satisfy the regularity condition at the event horizon; hence, the solution is naturally extended beyond the event horizon up to the singularity. Thus, if we restrict the situation to determine that our solution is formed from astrophysical processes, e.g., gravitational collapses, we can restrict our solutions above a timelike hypersurface (blue dashed curve) that may, for example, denote a star surface. So, the final physically sensible causal structure becomes right of Fig. 2.

III. PROPERTIES OF THE SCALAR HAIRY BLACK HOLES

We are interested in the Hawking temperature T_H and area of horizon A_H of these black holes,

$$T_H = \frac{1}{4\pi} N'(r_H) e^{-\sigma_H}, \qquad A_H = 4\pi r_H^2, \tag{24}$$

where σ_H is the value of function σ at the horizon. For the convenience of comparing our black hole solution with other known solutions, we introduce the following reduced quantities at the horizon of the black holes;

$$a_H = \frac{A_H}{16\pi M^2}, \qquad t_H = 8\pi T_H M. \tag{25}$$

The Ricci scalar R and Kretschmann scalar K for the black hole spacetime are given by the following:

$$R = -N'' + \frac{3r\sigma' - 4}{r} N' + \frac{2(2rN\sigma' - N + 1 + r^2 N\sigma'' - r^2 N\sigma'^2)}{r^2}, \tag{26}$$

$$K = (3\sigma' N' + 2N\sigma'' - N'' - 2N\sigma'^2)^2 + \frac{2}{r^2}(N' - 2N\sigma')^2 + \frac{2N'^2}{r^2} + \frac{4(N-1)^2}{r^4}. \tag{27}$$

With the series expansion of functions at the horizon, the R and K are finite with the leading order as follows:

$$R = -\frac{2m_1(3r_H\sigma_1 - 2)}{r_H^2} + \frac{3\sigma_1 + 4m_2}{r_H} + O(r - r_H), \tag{28}$$

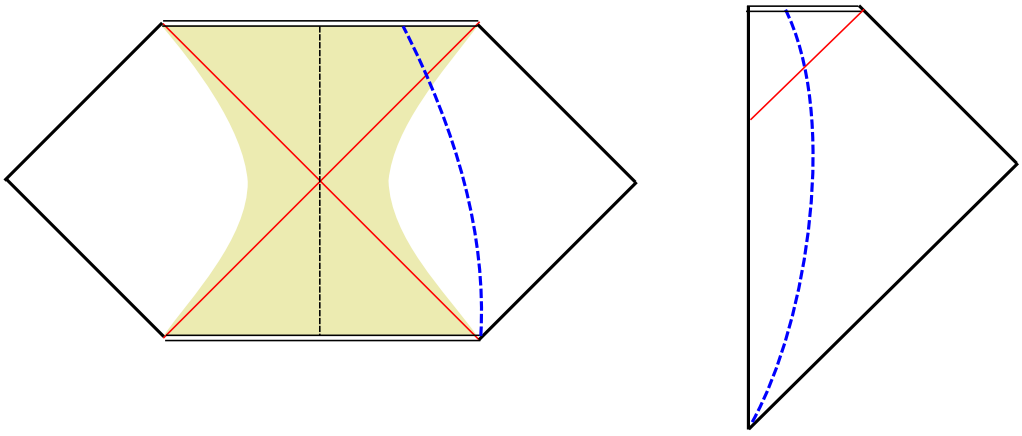

FIG. 2. Left: the maximally extended causal structure for hairy black holes. The yellow-colored part denotes a region for negative vacuum energy. The black dashed curve denotes a cusp surface of the scalar field, and the blue dashed curve denotes a star surface. Right: the physically sensible interpretation of the hairy black hole does not include any cusp region.

$$K = \frac{16m_2^2}{r_H^2} - \frac{8(-2+6m_1\sigma_1 r_H + 4m_1 - 3\sigma_1 r_H)}{r_H^3} + \frac{12 - 32m_1 + 48m_1^2\sigma_1 r_H + 36m_1^2\sigma_1^2 r_H^2 + 32m_1^2 + 9\sigma_1^2 r_H^2 + 12\sigma_1 r_H - 36\sigma_1^2 r_H^2 m_1 - 48m_1\sigma_1 r_H}{r_H^4} + O(r - r_H). \quad (29)$$

IV. THE RADIAL PERTURBATION

In the case of radial perturbation, we perturb the background metric and scalar field, respectively as [33]

$$ds^2 = -N(r)e^{-2\sigma(r)}[1 + \epsilon e^{-i\omega t}F_t(r)]dt^2 + \frac{1}{N(r)}[1 + \epsilon e^{-i\omega t}F_r(r)]dr^2 + r^2(d\theta^2 + \sin^2\theta d\varphi^2), \quad (30)$$

$$\Phi = \phi(r) + \epsilon\Phi_1(r)e^{-i\omega t}, \quad (31)$$

where $F_t(r)$, $F_r(r)$ and $\Phi_1(r)$ are the small perturbations to the nonperturbed solutions.

By substituting the above Ansatz to the Einstein equation and KG equation, we obtain a set of ODEs for the perturbation functions:

$$F_r = 8\pi G r\Phi_1\phi', \quad (32)$$

$$F_t' = -F_r' + 16\pi G r\Phi_1'\phi', \quad (33)$$

$$\Phi_1'' = \left(\sigma' - \frac{N'}{N} - \frac{2}{r}\right)\Phi_1' + \left(\frac{1}{N}\frac{d^2V}{d\phi^2} - \omega^2\frac{e^{2\sigma}}{N^2}\right)\Phi_1 + \frac{F_r}{N}\frac{dV}{d\phi} + \frac{F_r' - F_t'}{2}\phi'. \quad (34)$$

We observe that only Eq. (34) is independent because other ODEs [Eqs. (32) and (33)] are dependent. Hence, we transform Φ_1'' to a Schrödinger-like master equation by defining $Z(r) = r\Phi_1(r)$:

$$\frac{d^2Z}{dr_*^2} + (\omega^2 - V_R(r))Z = 0, \quad (35)$$

with the effective potential $V_R(r)$,

$$V_R(r) = Ne^{-2\sigma}\left[\frac{N}{r}\left(\frac{N'}{N} - \sigma'\right) - 8\pi G r N\phi'^2\left(\frac{N'}{N} + \frac{1}{r} - \sigma'\right) + 16\pi G r\phi'\frac{dV}{d\phi} + \frac{d^2V}{d\phi^2}\right]. \quad (36)$$

The tortoise coordinate r_* is

$$\frac{dr_*}{dr} = \frac{e^{\sigma}}{N}. \quad (37)$$

The perturbation Z is unstable when $\omega^2 < 0$ where the perturbation grows exponentially with time. In the compactified coordinate x, the effective potential V_R has the following expansions at the origin and horizon, respectively,

$$\text{Scalaron: } V_R(0) = \tilde{V}_0 + \tilde{V}_1 x + \tilde{V}_2 x^2 + O(x^3), \quad (38)$$

$$\text{Black Hole: } V_R(0) = \hat{V}_1 x + \hat{V}_2 x^2 + O(x^3), \quad (39)$$

where $\tilde{V}_i$ and $\hat{V}_i$ are constants that depend on the parameters of the background solution.

Note that Eq. (35) is an eigenvalue problem. Hence, we compute the radial mode numerically by using COLSYS to solve it with ω^2 as the eigenvalue. For black holes, we impose that the first-order derivative of the perturbation function vanishes at the boundaries, $\partial_r Z(r_H) = \partial_r Z(\infty) = 0$. In the case of the scalaron, we impose that the perturbation function vanishes at the boundaries. In the numerics, we introduce an auxiliary equation $\frac{d}{dr}\omega^2 = 0$, that allows us to impose an additional condition $Z(r_p) = 1$ at some point r_p, which typically lies in the middle of the horizon/origin and infinity. This allows us to obtain a nontrivial and normalizable solution for Z, because Eq. (35) is homogeneous. The eigenvalue ω^2 is found automatically when Z satisfies all the asymptotic boundary conditions.

V. RESULTS AND DISCUSSIONS

A. General properties and domain of existence

By fixing several values of global minimum ϕ_1, we exhibit the properties of hairy black holes, which are reduced area of horizon a_H and reduced Hawking temperature t_H in Fig. 3. The purpose of introducing these reduced quantities is to compare our hairy black holes with a known solution, which is the Schwarzschild black hole in this case. Recall that both a_H and t_H are unity for Schwarzschild black hole. By increasing the value of the scalar field at the horizon ϕ_H from zero, a branch of hairy black hole solutions emerges from the Schwarzschild black hole. As ϕ_H increases, a_H decreases from unity, and t_H increases from unity. When $\phi_H \to \phi_1$, a_H decreases to zero and t_H increases very sharply for $\phi_1 = 0.5$, 1.0. We could not generate configurations for $\phi_H = \phi_1$, the solutions becoming singular as we reach this value of the parameter. Note that when $\phi_H = \phi_1$, the scalar field sits exactly at the true vacuum ϕ_1 of the potential, and the tunneling effect does not occur.

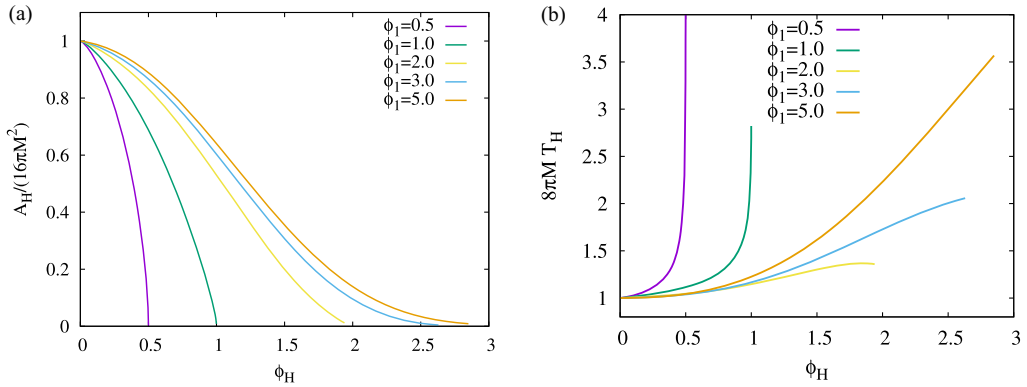

FIG. 3. The properties of hairy black holes $(r_H = 1, V_0 = 1)$ with several global minimum ϕ_1 as a function of ϕ_H: (a) The scaled area of horizon a_H. (b) The scaled Hawking temperature t_H.

For higher values of ϕ_1 (i.e. $\phi_1 = 2.0,\ 3.0,\ 5.0$), the reduced area a_H also decreases almost to zero but the reduced temperature t_H remains finite. Again, the solutions should become sick in the limit $\phi_H = \phi_1$, but numerically reaching this limit is more complicated, as the code stops working for values of ϕ_H slightly below ϕ_1 (for $\phi_1 = 2.0$, 3.0) and ϕ_H far below ϕ_1 (for $\phi_1 = 5.0$).

In Fig. 4 we show the relation between the mass of hairy black holes and scalarons with the value of ϕ_c. The scalaron solutions (purple curve) emerge from the Minkowski spacetime, where the mass is zero and the scalar field vanishes. As the value of the scalar field at the origin ϕ_c increases from zero, the mass of the scalaron also increases. When $\phi_c \to \phi_1$, the mass of the scalaron increases very sharply.

The color bars in the Fig. 4 represent the size of the black hole horizon, which indicate that the mass of scalaron relates to hairy black holes in the small horizon limit

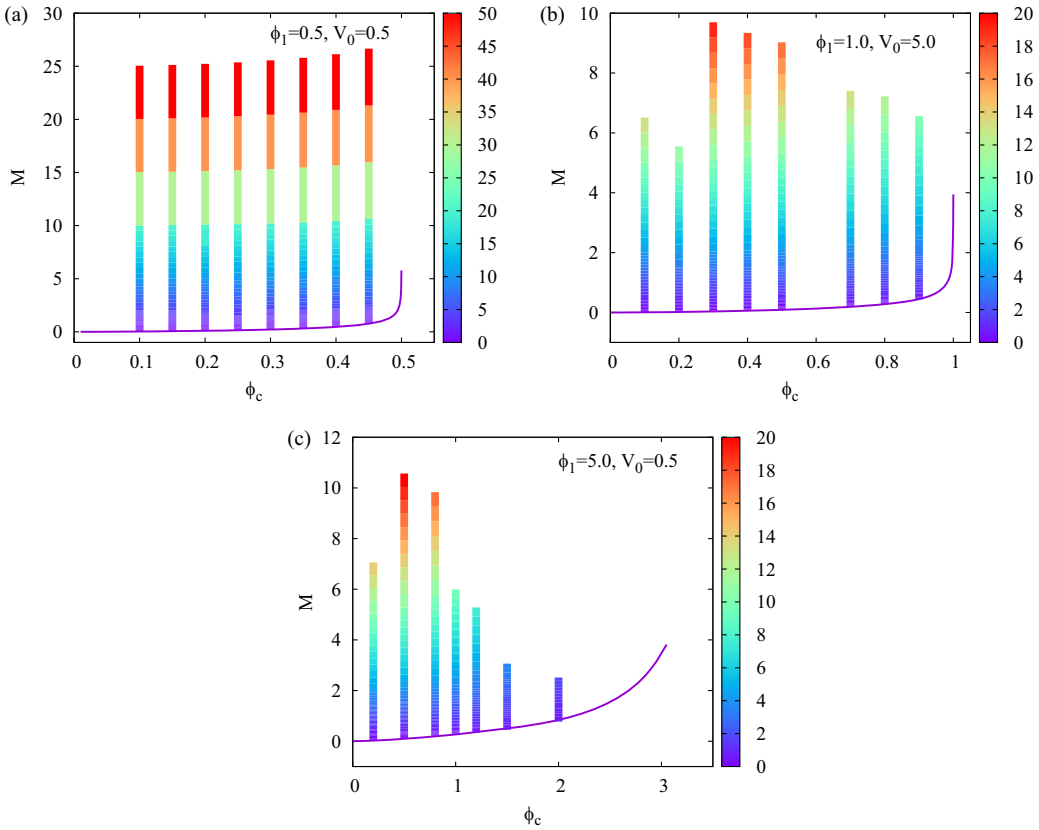

FIG. 4. The mass M as a function of the parameter ϕ_c for (a) $V_0 = 0.5, \phi_1 = 0.5$ (b) $V_0 = 5.0, \phi_1 = 1.0$ (c) $V_0 = 0.5, \phi_1 = 5.0$. The purple curve corresponds to the scalaron, and the rest of the colored lines are for sets of black holes with fixed values of ϕ_H (in this case $\phi_c = \phi_H$). The color gradient indicates the size of the horizon radius r_H.

$(r_H \to 0)$. Thus, the hairy black holes possess the scalaron as the limiting configuration in the small horizon limit. Analogous to the hairy black holes, for $\phi_1 = 0.5$, 1.0, the scalarons do not exist when $\phi_c = \phi_1$ as the scalar field ϕ_c sits exactly at the true vacuum ϕ_1. For large ϕ_1, e.g., $\phi_1 = 5.0$, the scalaron solutions are more difficult to generate numerically, and we cannot reach values of ϕ_c too close to ϕ_1.

We exhibit the typical profiles of solution in the compactified coordinate x for the hairy black holes and scalaron in Fig. 5. Both compact objects show a similar pattern for the functions. As the value of the scalar field at the horizon or the origin becomes closer to ϕ_1, these solutions become closer to bubbles of true vacuum surrounded by the false vacuum.

We observe that the solutions have almost constant functions in the bulk, corresponding (almost) to the global minimum of the potential, and thus the true vacuum ϕ_1. Moving away from the horizon, the solutions develop a sharp boundary at some intermediate region of the spacetime, where the functions rapidly change to another set of almost constant functions. This region corresponds to the imposed false vacuum $(a = 0)$ at infinity, where the scalar sits in the local minimum.

Moreover, the mass function $m(x)$ possesses a global minimum and can be strictly nonpositive [see Fig. 5(b)], which indicates the violation of the energy conditions. We observe that the global minimum of $m(x)$ decreases very sharply as ϕ_H increases to the limit value. This sharp behavior of the $m(r)$ function propagates into the metric component g_{rr}, which we display in Fig. 6. The global minimum of $m(x)$ gives rise to the global maximum of $N(x)$, since $N(x) = 1-2m(x)(1-x)/r_H$. Thus, the global maximum of $N(x)$ also gives rise to the global minimum of g_{rr} since $g_{rr} = 1/N(x)$.

To further illustrate how in the limit the spacetime is divided into two different regions dominated by the two possible vacua, in Fig. 7 we show the profiles of the scalar field for hairy black holes and scalarons. As ϕ_H and ϕ_c increase to ϕ_1, the scalar field profile becomes closer and closer to a step function: the bulk region possesses the value of the true vacuum ϕ_1, whereas the exterior region possesses the value of the false vacuum $(a = 0)$.

The Ricci scalar R and Kretschmann scalar K for a hairy black hole with $\phi_1 = 1.0$ are shown in Figs. 8(a) and 8(b), respectively. The Ricci scalar at the horizon decreases from zero to some negative values when ϕ_H increases. This indicates that the bulk of the hairy black hole

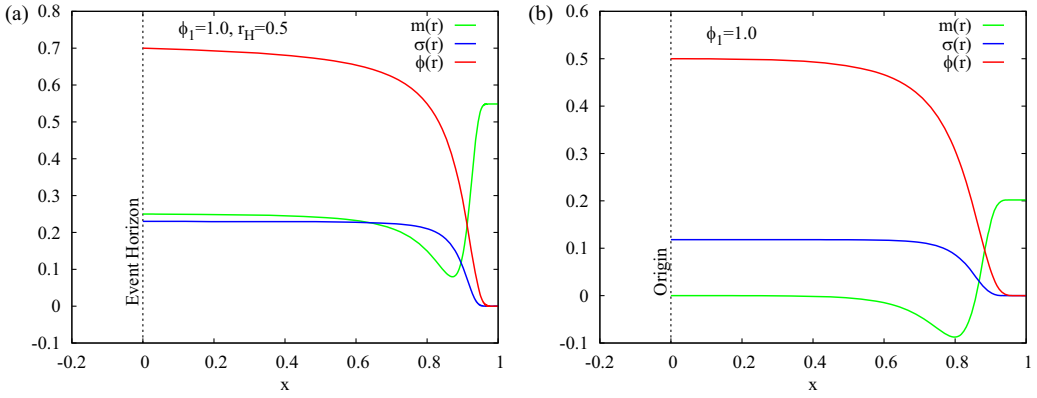

FIG. 5. Typical profiles of the functions in the compactified coordinate x for (a) black holes. (b) scalaron.

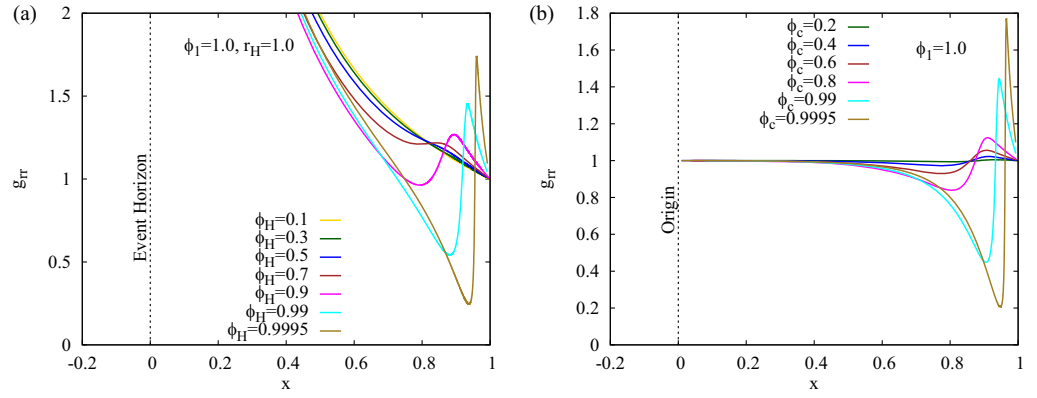

FIG. 6. The metric component g_{rr} for (a) hairy black hole (b) scalaron in the compactified coordinate x.

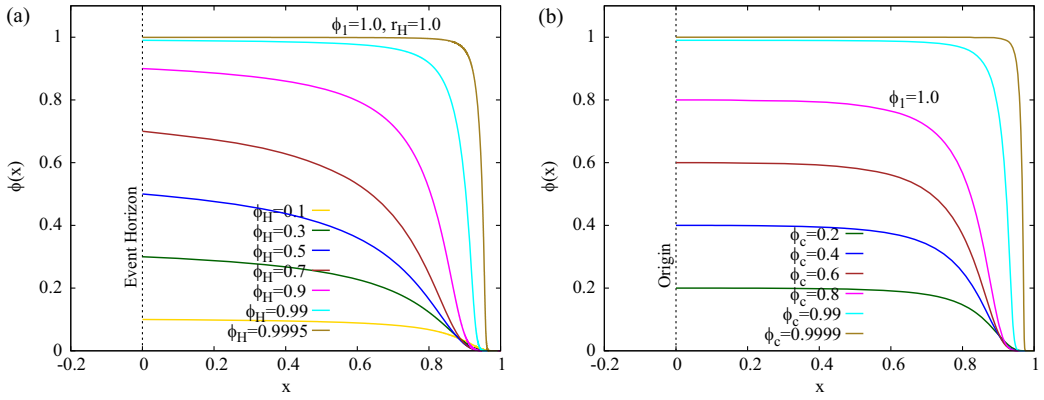

FIG. 7. Profiles of the scalar field ϕ for (a) hairy black hole (b) scalaron in the compactified coordinate x.

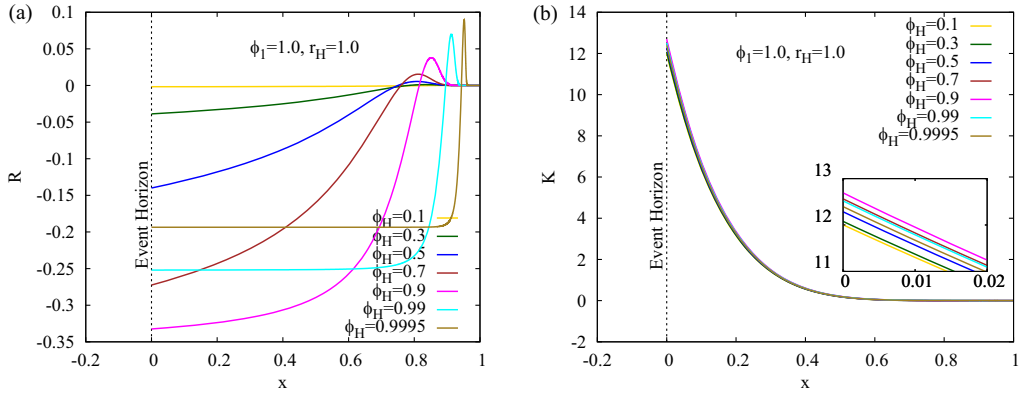

FIG. 8. (a) The Ricci scalar and (b) The Kretschmann scalar for a hairy black hole in the compactified coordinate x.

possesses negative curvature. From the horizon to a point where the functions have a sharp boundary, the profile of R increases from a negative value to zero and then to a positive value, before fallings to zero again at infinity. However, the Kretschmann scalar is positive at the horizon, and its profile decreases monotonically to zero at infinity.

B. Spherical stability

In Fig. 9, we show the effective potential V_R in the compactified coordinate for the scalaron and hairy black holes. V_R possesses finite value at the origin for scalaron but V_R is zero for the hairy black holes. In this figure, the potential always possesses a negative region for both types of objects, indicating the existence of instability.

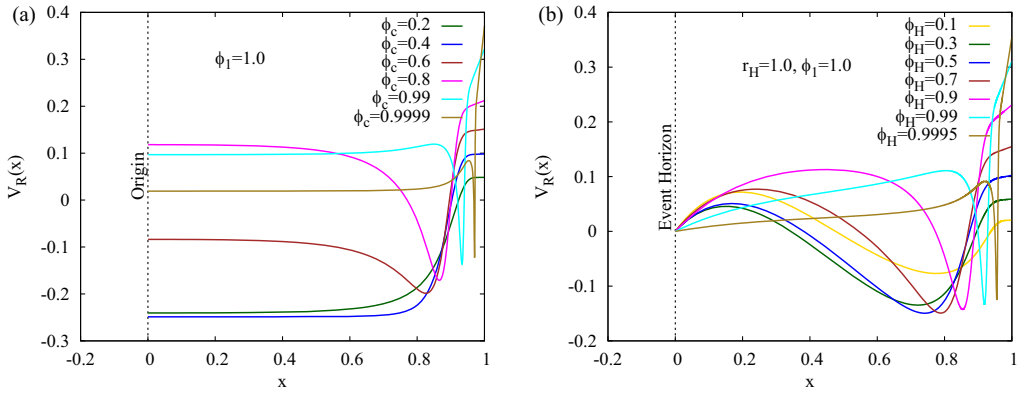

FIG. 9. Typical profile of the effective potential $V_R(x)$ in the compactified coordinate x for (a) scalaron (b) black holes. In color, we plot the potential for different values of the ϕ_c parameter.

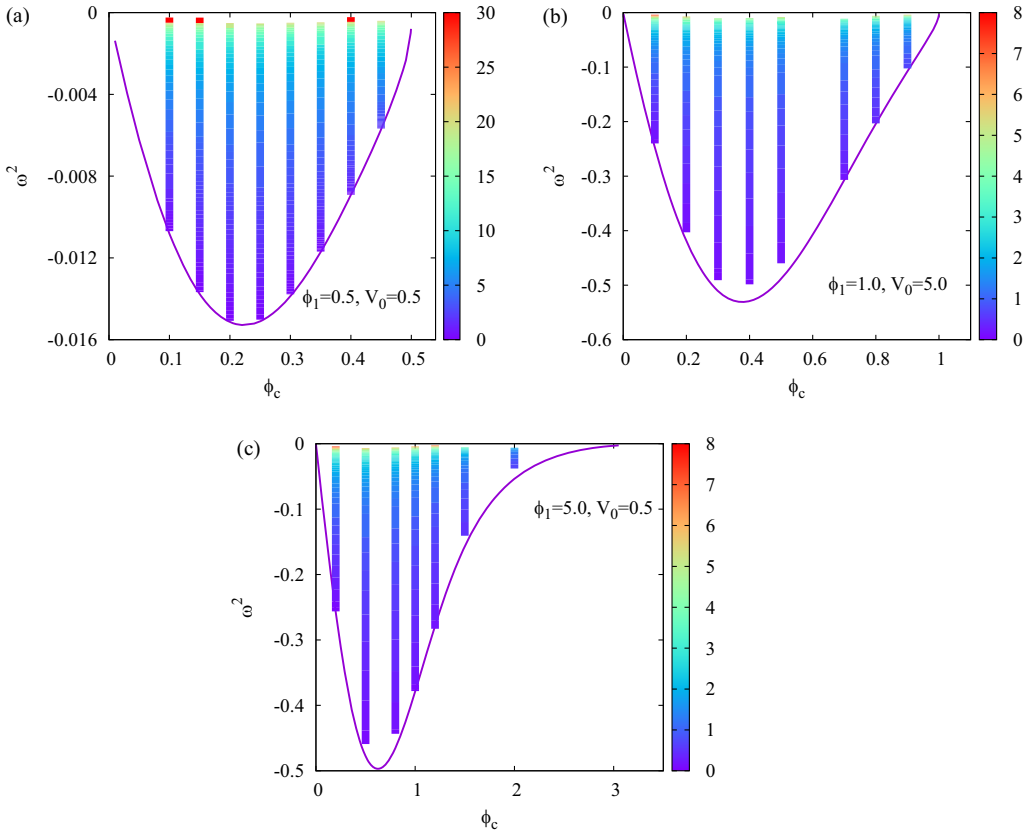

FIG. 10. The eigenvalue ω^2 as a function of the parameter ϕ_c. The purple curve corresponds to the scalaron, and the rest of the colored lines are for sets of black holes with fixed values of ϕ_H (in this case $\phi_c = \phi_H$). The color gradient indicates the size of the horizon radius r_H.

In fact, it is possible to obtain unstable radial modes for all the solutions we have studied. In Fig. 10 we exhibit the spectra of unstable radial modes for hairy black holes and scalarons as a function of the ϕ_c parameter. The unstable modes decrease from zero to a minimum value as this parameter is increased. From the minimum, the unstable mode increases again as ϕ_c approaches the value of ϕ_1 (the numerical results indicate that the mode becomes zero exactly at this value, not before). The modes for hairy black holes and scalarons are also smoothly connected in the small horizon limit. Interestingly we find that the unstable mode of the hairy black holes decreases in magnitude with the size of the horizon. This indicates that black holes with large horizon sizes could be effectively stable (at least in some timescale).

Such instability is not so surprising, because our solution is a kind of spherical symmetric true vacuum bubbles in the false vacuum background. The scalar field configuration between the black hole and the asymptotic infinity can be interpreted as a domain wall, while the domain wall will expand over the false vacuum background. It is worthwhile to mention that we have shown a nontrivial true vacuum bubble solution in the spherical symmetric background that is rather complicated than $O(4)$-symmetric cases.

VI. CONCLUSION

The gravity minimally coupled to a scalar potential allows the construction of hairy black holes by requiring the scalar potential to be nonstrictly positive for violating the energy conditions [7]. Reference [8] employed such scalar potential which has a global minimum ϕ_1, a local minimum a, and a local maximum ϕ_0 to construct the spherically symmetric and asymptotically flat hairy black holes and study their empirical mass formulas. The asymptotic flatness condition of black holes is guaranteed by fixing the local minimum of the potential to zero. This potential has been widely applied to study the quantum tunneling process from the false vacuum a to the true vacuum ϕ_1 in cosmology.

In this study, we performed a comprehensive study of the properties of black holes by solving the Einstein-matter field equations numerically. We fixed the global minimum (true vacuum) and varied the value of the scalar field at the horizon ϕ_H to generate the hairy black holes solutions. Thus, a branch of hairy black holes with fixed horizon size emerged from the Schwarzschild black holes. For small ϕ_1, when ϕ_H increased from zero and approached ϕ_1, the scaled area of horizon decreased from unity to zero and the scaled Hawking temperature increased very sharply from

unity. In the limit $\phi_H = \phi_1$, the scalar field sat exactly at the true vacuum ϕ_1 and no tunneling occurred; thus, hairy black holes did not exist anymore in that limit. For large ϕ_1, the scaled area of horizon also decreased from unity to zero, but the scaled Hawking temperature increased to a finite value from unity when ϕ_H increased to a value that was still less than ϕ_1. In such a situation, we were unable to generate the solutions for ϕ_H beyond that value because the numerical code stops working.

Analogous to the hairy black holes, a branch of globally regular particle-like solution that is known as scalaron emerged from the Minkowski spacetime by varying the scalar field at the origin ϕ_c. The scalaron also behaved analogously with the hairy black holes in the limit $\phi_c = \phi_1$ where the mass increased very sharply. Similarly, we were also unable to generate the scalaron for large ϕ_1. In addition, the hairy black holes were reduced to the scalaron in the small horizon limit.

The profiles of both compact objects behaved similarly; they had almost constant functions in the bulk, which corresponded to the true vacuum ϕ_1, before showing a sharp boundary where the functions rapidly changed to another set of constant functions which corresponded to the false vacuum ($a = 0$) that lies at the infinity.

We also investigated the linear stability of hairy black holes by performing the radial perturbation on the metric and scalar fields. Hence, we obtained a master equation which is Schrödinger-like. We numerically solved the master equation to compute the spectra of radial modes. Generically, both hairy black holes and scalaron are unstable against the radial perturbation. Both spectra decrease from zero to a minimum value and then increased to zero as the value of the scalar field increased from zero and then approached ϕ_1. Moreover, the unstable modes of hairy black holes are connected with scalaron in the small horizon limit. We also found that the hairy black holes with larger horizon sizes are relatively stable against the perturbation.

There are many possible directions that can be derived from this study. One possibility is to consider theories that allow for a nonminimally coupled scalar field with the Ricci scalar [9]. It would be interesting to study the properties of the hairy black holes in these models, and in particular, analyze the influence of the nonminimal coupling in the radial instability. This requires a more rigorous calculation and analysis that we shall report in the future. In addition, we can consider studying the properties of charged hairy black holes for this model and their linear stability. It is also interesting to generalize these static hairy black holes to the rotating hairy black holes so that we can study the difference between the properties of rotating hairy black holes with Kerr black holes.

ACKNOWLEDGMENTS

D.Y. and X. Y. C. are supported by the National Research Foundation of Korea (Grants No. 2021R1C1C1008622, No. 2021R1A4A5031460). X. Y. C. is grateful for the hospitality from the organizer at APCTP in Pohang to present this work in the workshop String theory, Gravity, and Cosmology (SGC2022). J. L. B. S. gratefully acknowledges support from MICINN Project No. PID2021-125617NB-I00, Santander-UCM Project No. PR44/2129910, DFG Research Training Group 1620 *Models of Gravity* and FCT Project No. PTDC/FIS-AST/3041/2020. We are grateful to have had a useful discussion with Jutta Kunz.

[1] R. Bartnik and J. Mckinnon, Phys. Rev. Lett. **61**, 141 (1988).
[2] P. Bizon, Phys. Rev. Lett. **64**, 2844 (1990).
[3] M. S. Volkov and D. V. Galtsov, Sov. J. Nucl. Phys. **51**, 747 (1990).
[4] H. P. Kuenzle and A. K. M. Masood- ul- Alam, J. Math. Phys. (N.Y.) **31**, 928 (1990).
[5] B. R. Greene, S. D. Mathur, and C. M. O'Neill, Phys. Rev. D **47**, 2242 (1993).
[6] G. V. Lavrelashvili and D. Maison, Nucl. Phys. **B410**, 407 (1993).
[7] C. A. R. Herdeiro and E. Radu, Int. J. Mod. Phys. D **24**, 1542014 (2015).
[8] A. Corichi, U. Nucamendi, and M. Salgado, Phys. Rev. D **73**, 084002 (2006).
[9] U. Nucamendi and M. Salgado, Phys. Rev. D **68**, 044026 (2003).
[10] O. Bechmann and O. Lechtenfeld, Classical Quantum Gravity **12**, 1473 (1995).
[11] H. Dennhardt and O. Lechtenfeld, Int. J. Mod. Phys. A **13**, 741 (1998).
[12] K. A. Bronnikov and G. N. Shikin, Gravitation Cosmol. **8**, 107 (2002).
[13] C. Martinez, R. Troncoso, and J. Zanelli, Phys. Rev. D **70**, 084035 (2004).
[14] E. Winstanley, Classical Quantum Gravity **22**, 2233 (2005).
[15] V. V. Nikonov, J. V. Tchemarina, and A. N. Tsirulev, Classical Quantum Gravity **25**, 138001 (2008).
[16] A. Anabalon and J. Oliva, Phys. Rev. D **86**, 107501 (2012).
[17] C. Gao and J. Qiu, Gen. Relativ. Gravit. **54**, 158 (2022).
[18] T. Karakasis, E. Papantonopoulos, Z. Y. Tang, and B. Wang, Eur. Phys. J. C **81**, 897 (2021).
[19] S. R. Coleman and F. De Luccia, Phys. Rev. D **21**, 3305 (1980).

[20] A. Masoumi and E. J. Weinberg, Phys. Rev. D **86**, 104029 (2012).
[21] P. Burda, R. Gregory, and I. Moss, J. High Energy Phys. 06 (2016) 025.
[22] V. De Luca, G. Franciolini, and A. Riotto, Phys. Rev. D **104**, 123539 (2021).
[23] L. Perivolaropoulos and F. Skara, Phys. Rev. D **107**, 083509 (2023).
[24] J. Braden, M. C. Johnson, H. V. Peiris, A. Pontzen, and S. Weinfurtner, Phys. Rev. D **107**, 083509 (2023).
[25] A. Ekstedt, Phys. Rev. D **106**, 095026 (2022).
[26] J. S. Cruz, S. Brandt, and M. Urban, Phys. Rev. D **106**, 065001 (2022).
[27] S. Vicentini, arXiv:2205.11036.
[28] A. Kosowsky, M. S. Turner, and R. Watkins, Phys. Rev. D **45**, 4514 (1992);
[29] D. H. Kim, B. H. Lee, W. Lee, J. Yang, and D. Yeom, Eur. Phys. J. C **75**, 133 (2015).
[30] B. H. Lee, W. Lee, D. h. Yeom, and L. Yin, Chin. Phys. C **46**, 075101 (2022).
[31] R. Gregory, I. G. Moss, and N. Oshita, J. High Energy Phys. 07 (2020) 024.
[32] U. Ascher, J. Christiansen, and R. D. Russell, Math. Comput. **33**, 659 (1979).
[33] J. L. Blázquez-Salcedo, C. A. R. Herdeiro, J. Kunz, A. M. Pombo, and E. Radu, Phys. Lett. B **806**, 135493 (2020).